Geologic origin of the source of Bearhead Rhyolite (Paliza Canyon) obsidian, Jemez Mountains, Northern New Mexico

M. Steven Shackley[1],* *Fraser Goff*[2], *Sean G. Dolan*[3]
[1]Geoarchaeological XRF Laboratory, Albuquerque, New Mexico, and Department of Anthropology, University of New Mexico, Albuquerque 87171, *shackley@berkeley.edu*
[2]Department of Earth and Planetary Sciences, University of New Mexico, Albuquerque 87171
[3]Los Alamos National Laboratory, Los Alamos, NM 87545
*Corresponding author: *shackley@berkeley.edu*

Abstract

Recent field and analytical studies of what has been traditionally called "Paliza Canyon obsidian" in the archaeological vernacular show it to be Bearhead Rhyolite that is part of the Late Tertiary (Neogene) Keres Group of the Jemez Mountains, northern New Mexico. The geological origin of all other archaeological obsidian sources in the Jemez Mountains have been reported and are well documented in the literature. But the so-called "Paliza Canyon" source, important as a toolstone to Pueblo Revolt Colonial period occupants of the Jemez Mountains area and present in regional archaeological contexts throughout prehistory, had remained unlocated and undocumented. The Bearhead Rhyolite origin for the "Paliza Canyon" obsidian (which we suggest should now be named "Bearhead Rhyolite") solves this ambiguity and provides more precise geological and geographical data for archaeological obsidian source provenance in the region.

Introduction

An important type of obsidian used by Native Americans, traditionally called the "Paliza Canyon" obsidian (Nelson 1984; Baugh & Nelson 1987; Wolfman 1994; Glascock et al., 1999; Shackley 2005), is widespread in the archaeological record in New Mexico. Church (2000) and Shackley (2012a) have both reported the presence of Paliza Canyon obsidian in Rio Grande Quaternary alluvium as far south as Las Cruces, New Mexico. It also occurs commonly in Pueblo Revolt period archaeological sites (late 17th century) in the southern Jemez Mountains of northern New Mexico, including near Jemez Springs (Fig. 1; Liebmann 2012; Shackley 2009a, 2012b). Using x-ray fluorescence spectrometric (XRF) analyses, these archaeological samples have been chemically correlated to a "Paliza Canyon" geologic source defined in the Baugh and Nelson (1987) study. XRF is the preferred method for chemically characterizing archaeological obsidian because it is relatively inexpensive and can be accomplished non-destructively (Shackley 2005, 2011). Determining the eruptive location of this unique archaeological obsidian is crucial for understanding exchange, migration, and social networks during the Pueblo Revolt period (A.D. 1680–1692), as well as all prehistoric through Colonial periods in New Mexico (Liebmann 2012; Shackley 2005).

The original four samples of "Paliza Canyon" obsidian were collected in a portion of Paliza Canyon, a drainage located in the southern Jemez Mountains (Figs. 1–2, near our sample locality 100915-2; Nelson 1984; Baugh and Nelson 1987). It is important to note that these samples were from late Quaternary, valley bottom alluvium and thus geologically reworked. The goal of our study was to locate the primary geologic source of these samples.

The original "Paliza Canyon" source was characterized as a small-nodule Neogene source, based on the age of adjacent volcanic rocks and small nodule sizes (as opposed to large nodule Quaternary sources, such as Valles Rhyolite obsidian). The small nodule sizes likely reflect hydration and perlitization of volcanic glass over relatively long periods of geologic time. Known Neogene and Quaternary sources of archaeological obsidian in the Jemez Mountains have been well dated and chemically, stratigraphically, and isotopically studied for a number of years. The geologic context of the "Paliza Canyon" obsidian has been more difficult to decipher because of complexities in its geochemistry and geologic setting (compounded by its relatively old age), especially when compared with most other Jemez Mountains sources (Gardner et al., 1986; Self et al., 1986; Spell and Harrison 1993; Ellisor et al., 1996; Goff et al., 1996; Kues et al., 2007; Kelley et al., 2013).

Relatively recent geologic mapping and sampling efforts in the southern Jemez Mountains, combined with XRF analyses of several samples, indicate that the primary source for the "Paliza Canyon obsidian" is only a few kilometers north of the original proposed source area. After providing a geologic background, we use geochemical data to compare the "Paliza Canyon obsidian" with possible primary geologic sources in the area. We argue that the best candidate for a primary source is a geologic unit called the Bearhead Rhyolite. To be consistent with our interpretations, in the rest of the paper we refer to the archeological artifacts previously called "Paliza Canyon obsidian" as the Bearhead Rhyolite obsidian.

Geologic background of study area

Our study area (Figs. 1, 2) encompasses both our new sampling localities and the Paliza Canyon sampling area of Nelson (1984) and Baugh and Nelson (1987). In this area, obsidian occurs in three types of geologic units (Fig. 2): 1) surficial, relatively weakly consolidated tephra, 2) in valley-bottom alluvium, and 3) volcanic bedrock. In the study area, most surficial tephra is petrographically similar to what is now called the El Cajete Pyroclastic Beds of the East Fork Member of Valles Rhyolite (Gardner et al., 2010; Goff et al., 2011), which we simply refer to as El Cajete pumice, whose age is interpreted as 74.7±1.3 ka

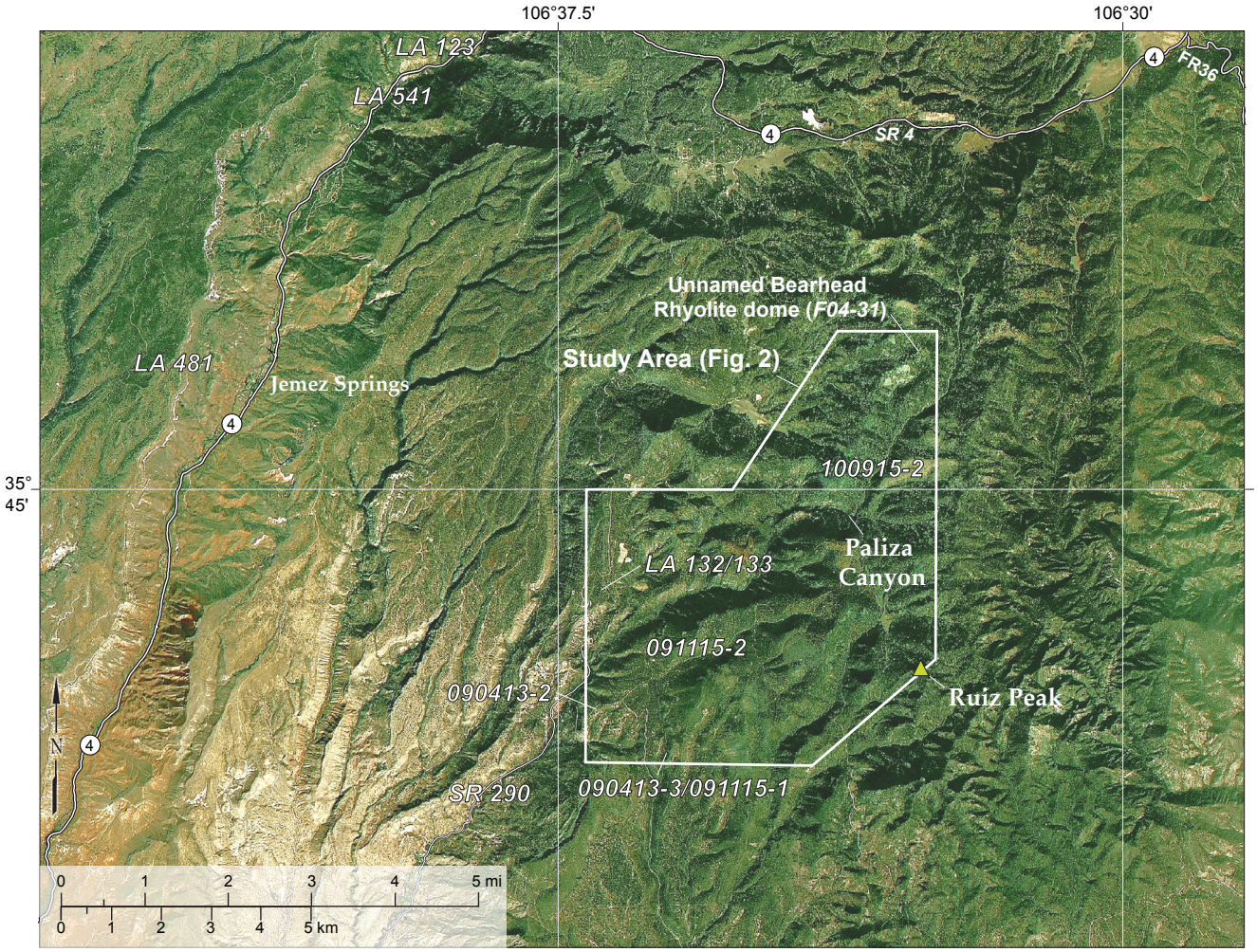

Figure 1. Orthophoto over digital elevation model. Study area depicted by polygon. Labels show approximate location of collection localities (i.e. 090413–2, 100915-2, etc.), geographic features, USGS quadrangle borders (in light gray), and Pueblo Revolt archaeological sites (LA numbers) near our study area (Liebmann 2012; Shackley 2009a, 2012b). Our precise collection localities are shown in Figure 2. Abbreviations: SR = state highway; FR = Santa Fe National Forest route.

(Zimmerer et al., 2016). However, in places the El Cajete pumice is so thin that underlying tephras from older volcanic bedrock locally crop out at the surface, as discussed below. Geologically reworked obsidian is abundant in late Quaternary alluvium filling Paliza Canyon proper, near the boundary of the Redondo Peak and Bear Springs Peak Quadrangles (Fig. 2). The "Paliza Canyon" obsidian sampled by Baugh and Nelson in the 1980s very likely came from late Quaternary, valley-bottom alluvium at this locality (Baugh and Nelson 1987; Tim Baugh, personal communication, 2015).

Volcanic bedrock obsidian localities are in 6–8 Ma lavas and volcaniclastic sediments. These volcanic units include the Bearhead Rhyolite and Paliza Canyon Formation. The Bearhead Rhyolite consists of more than 50 felsic domes, flows, dikes and sills emplaced throughout the Jemez Mountains (Kelley et al., 2013). Exposures with obsidian from the Bearhead Rhyolite are located just to the north of the aforementioned collection areas, one of which is the F04–31 dome of Goff et al., (2006) (labeled in northeast corner of Fig. 2). The obsidian commonly comes in the form of marekanites (also referred to as "Apache tears"), which are aphyric vitreous remnants in a rhyolitic perlite that commonly erode into subrounded-rounded pebbles (Lajčáková and Kraus 1993)." An $^{40}Ar/^{39}Ar$ age of 7.62 ± 0.44 Ma was obtained from an obsidian marekanite sample from this dome (Fig. 3; Goff et al., 2006; Kelley et al., 2013). Other Bearhead Rhyolite domes and flows in the vicinity yield ages ranging between 6.0 and 7.2 Ma (Justet 1996; Kempter et al., 2004).

In contrast to the felsic Bearhead Rhyolite, the volcanic domes and flows in the Paliza Canyon Formation are all mafic to intermediate composition (Ellisor et al., 1996; Goff et al., 2011; Kempter et al., 2004). Beneath the aforementioned (often very thin) blanket of El Cajete pumice are irregular beds of volcaniclastic conglomerates and associated pumiceous deposits (Tpv in Fig. 2) derived primarily from andesitic to dacitic rocks of the Paliza Canyon Formation (Kempter et al., 2004; Goff and Gardner 2004; Goff et al., 2006, 2011). These conglomerates contain older tephras and obsidian.

Sampling and field observations of obsidian sources

Obsidian sampling efforts were undertaken in September of 2013 and September–October of 2015. The first trip was mainly a reconnaissance. In the Fall of 2015, we

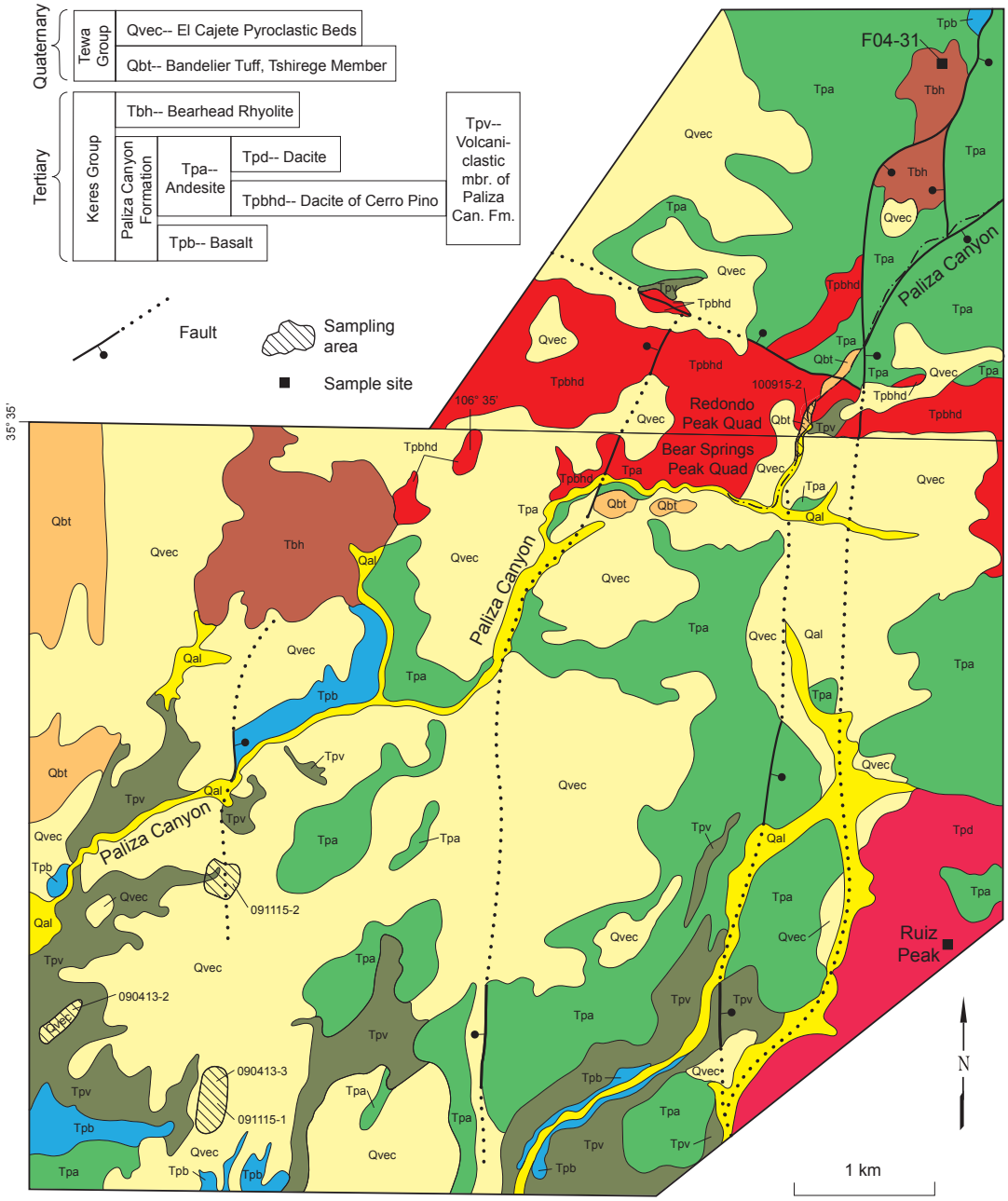

Figure 2. Simplified geologic map of the upper Paliza Canyon area, southern Jemez Mountains, New Mexico (modified from Kempter et al., 2004, and Goff et al., 2006; labels and terminology from Goff et al., 2011). Qal (dark yellow) = valley bottom alluvium. Qvec (pale yellow) = El Cajete Pyroclastic Beds; moderately sorted beds of rhyolitic pyroclastic fall and thin pyroclastic flow deposits (74.7±1.3 ka, Zimmerer et al., 2016); locally the beds are extremely thin. Qbt (orange) = Tshirege Member, Bandelier Tuff; rhyolitic ignimbrite (1.25±0.01 Ma, Phillips et al., 2007). Tpv (olive green) = volcaniclastic deposits, debris flows, hyper-concentrated flows, and stream deposits of the Paliza Canyon Formation. Tbh (reddish brown) = Bearhead Rhyolite; domes and flows of aphyric to slightly porphyritic lava (dome in northern Bear Springs Peak Quadrangle is 6.66±0.06 Ma, Kempter et al., 2004; faulted dome in Redondo Peak Quadrangle is 7.62±0.44 to 7.83±0.26 Ma, Goff et al., 2006). Tpa (green) = Paliza Canyon Fm, andesite, undivided; lava flows containing plagioclase and pyroxene (8.78±0.14 to 9.44±0.21 Ma, Justet 2003). Tpd (rose) = Paliza Canyon Fm. dacite; domes and flows of very porphyritic lava near Ruiz Peak. Tpbhd (red) = Paliza Canyon Fm. porphyritic biotite-hornblende dacite; dome and flows are 9.24±0.22 Ma (Justet 2003). Tpb (blue) = Paliza Canyon Fm. basalt; lava flows mostly containing visible olivine (9.45±0.07 to 9.54±0.08 Ma, Goff et al., 2006 and Kempter et al., 2004).

conducted sampling in order to compare the compositions of newly identified obsidian sources (e.g., Kempter et al., 2004) with the older "Paliza Canyon" source locale reported in Baugh and Nelson (1987). Figure 2 depicts our sampling localities (e.g., 090413–3); individual samples collected at a locality are denoted by a hyphen and numeral appended to the locality name (e.g., 090413–3–2, 090413–3–3).

On September 11, 2015, we examined geological localities in the northwest corner of the Bear Springs Peak 7.5' USGS Quadrangle to better understand the geological context of obsidian marekanites initially observed in mapping by Kempter et al., (2004) and in field reconnaissance. Because it contained obsidian clasts, the El Cajete pumice as mapped by Kempter et al., (2006) was initially considered by us as a possible source for the Bearhead Rhyolite obsidian. We confirmed that marekanites there only occurred in association with pyroclastic deposits, at that time thought to be El Cajete pumice. This pumice and accompanying obsidian was sampled at various localities (091115–2, 090413–2, 090413–3, 091115–1 in Fig. 2). The largest marekanite

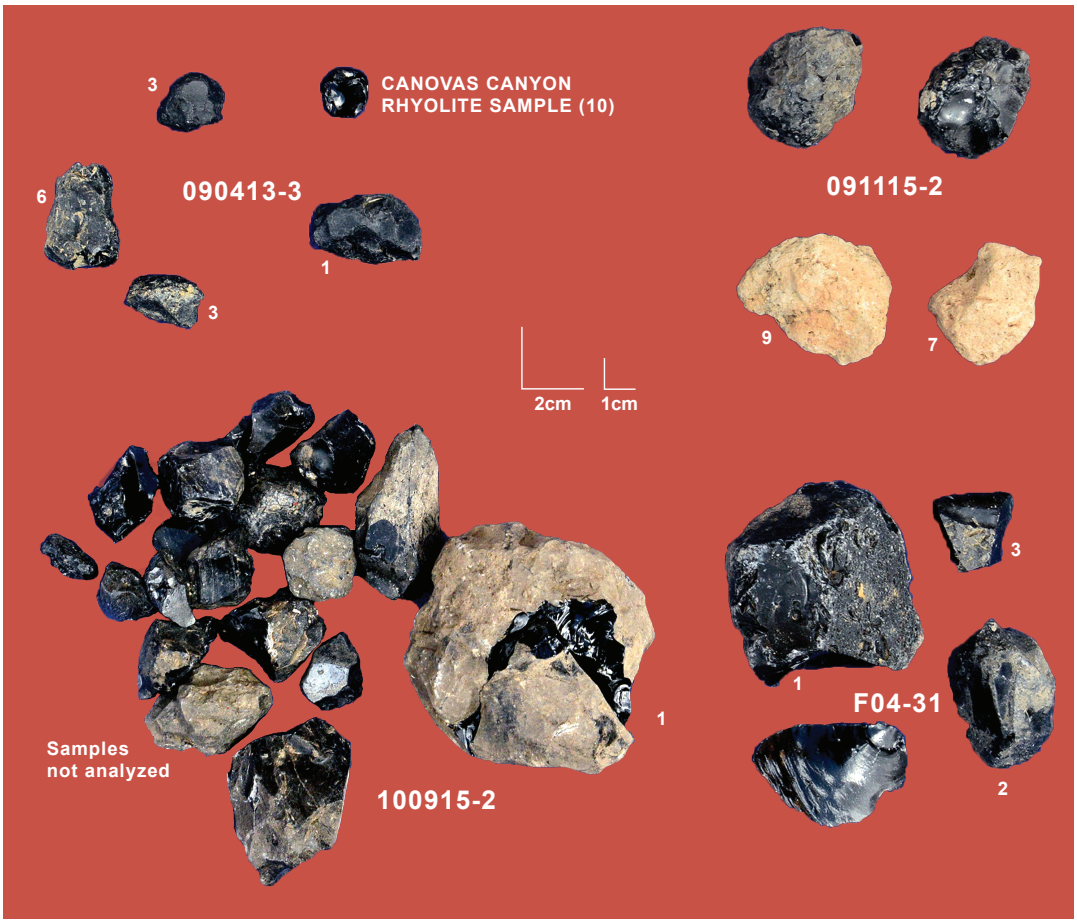

Figure 3. Photograph of Bearhead Rhyolite obsidian and dacite pumice samples by collection localities and sample numbers (see Figs. 1 and 2, and Table 2). Note general decrease in angularity and marekanite size from primary dome (F04–31), to secondary samples (locality 100915–2) in downstream alluvium in Paliza Canyon 2–3 km southwest of F04–31, locality 091115–2 above Paliza Canyon, and locality 090413–3 farther south (see Figs. 1 and 2). Samples listed in locality 100915–2 exclude analyzed samples in Table 2 from site 100915–2. Dacite pumice corresponds to samples 091115-2-7 and 091115-2-9.

recovered was 55.1 mm (long axis) but most were 10–30 mm, with a few 30–40 mm.

The Redondo Peak 7.5' USGS Quadrangle in Paliza Canyon was visited in October of 2015. There, we collected reworked (secondary deposit) obsidian in Paliza Canyon alluvium near the boundary between the Redondo Peak and Bear Springs Peak 7.5' USGS Quadrangles (locality 100915–2). This locality approximately corresponds with the original "Paliza Canyon" source locale (Baugh and Nelson 1987) and lies below and 2 to 3 km southwest of the unnamed dome informally called F04–31 (Figs. 1 and 2; Goff et al., 2006; Kelley et al., 2013). In the Paliza Canyon alluvium, we recovered a nearly 100 mm-long obsidian nodule and found abundant (100s per 5m^2) obsidian marekanites (see sample 100915–2 in Figure 3). Many of the marekanites were around 50 mm in diameter (Fig. 3). The purpose of the pumice samples was to determine if their composition was rhyolitic (and thus Bearhead Rhyolite) or dacitic (and thus part of the Paliza Canyon Formation).

XRF analyses

We used XRF to determine the chemical composition of these obsidian samples and tephra from the Paliza Canyon Formation. XRF analytical instrument methodology is detailed in Appendix 1 (see also Shackley 2005). Major oxide results are presented in Table 1 and Figure 4, and Table 2 lists selected trace element concentrations. In Table 3, we compare the mean and central tendency for the trace element data of our samples with those of Baugh and Nelson's (1987) original study.

Of primary importance to our study is the compositional similarity of the F04–31 rhyolite dome with alluvial obsidian samples collected at the "Paliza Canyon" source locality. This similarity is especially evident in the overlap of trace element concentrations (Table 2) between samples 100915–2–n ("Paliza Canyon" source locality) and F04–31–n (Bearhead Rhyolite dome). The mid-Z incompatible elements (Rb, Sr, Zr) most frequently used in geoarchaeological studies are generally similar, with minor differences in mean elemental concentrations (Table 3) attributable to changes in analytical technology since the 1980s (see Shackley 2011). Specifically, modern Si(Li) and SDD EDXRF detectors are more sensitive than the earlier WXRF instruments used for Baugh and Nelson's (1987) four samples (Shackley 2011). Figures 5 and 6 nicely illustrate this overlap between the two localities (100915-2 and F04-31) for Nb, Y, Ba concentrations. Thus, we interpret that the F04–31 dome is the source for the downstream alluvial obsidian clasts found in the "Paliza Canyon" source locality of Baugh and Nelson (1987). Note the relatively high Sr and Ba values of samples correlative to the Bearhead Rhyolite (brown,

TABLE 1. Major and minor oxide data for pumice, obsidian, and lava rock samples.

Sample	SiO_2	Al_2O_3	CaO	Fe_2O_3	K_2O	MgO	MnO	Na_2O	TiO_2	Σ
091115-2-7[1]	67.96	17.06	1.29	5.74	3.81	1.07	0.13	1.91	0.78	99.74
091115-2-8[1]	64.06	19.70	1.49	7.002	3.82	1.16	0.08	1.66	0.71	99.69
091115-2-9[1]	68.61	15.73	1.65	5.93	3.72	1.35	0.08	1.83	0.72	99.62
090413-3-2[2]	74.67	13.10	0.89	1.48	5.42	0.21	0.13	3.37	0.28	99.55
Banco Bonito F82-7[3]	73.9	13.6	1.59	1.86	4.15	0.64	0.05	3.87	0.29	99.95
El Cajete F82-6[4]	72.8	14.0	1.87	2.11	4.16	0.78	0.05	3.84	0.33	99.94
Paliza Cyn dacite[5]	68.99	13.35	2.62	3.84	2.96	0.77	0.09	3.97	0.74	99.75
RGM-1 (this study)	75.68	12.48	1.30	1.81	4.55	<0.1	0.04	3.77	0.20	99.82
RGM-1 USGS recommended	73.4	13.7	1.15	1.86	4.30	0.28	0.036	4.07	0.27	99.06

[1] Pumice samples associated with obsidian localities formerly mapped as El Cajete pumice above and east of Paliza Canyon (Kempter et al., 2004).
[2] Obsidian sample from an area formerly mapped as El Cajete pumice above and east of Paliza Canyon (Kempter et al., 2004)
[3] from Gardner et al. (1986)
[4] from F. Goff (unpub. data)
[5] from Ellisor et al. (1996)
Data not normalized to USGS recommended values.

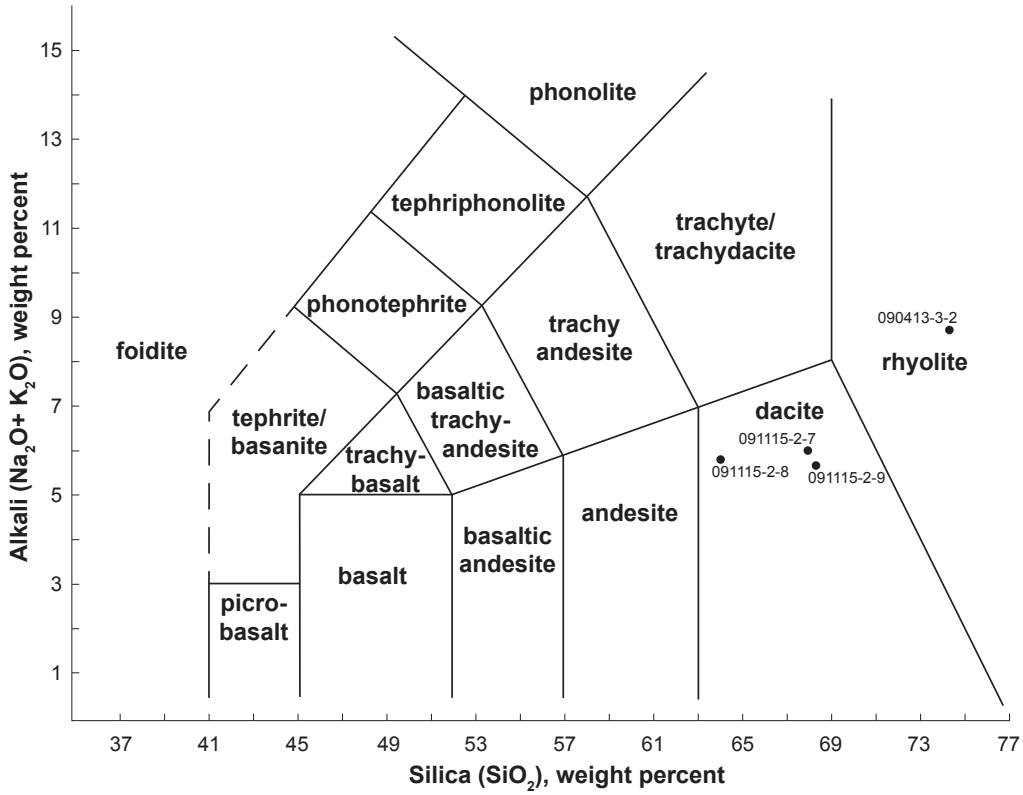

Figure 4. TAS plot (Le Bas et al., 1986) of selected samples in this study from Table 1. The elemental and major oxide data in Table 1 and this TAS plot demonstrate that some of the pumice in our study area is dacitic and probably from the volcaniclastic member of the Paliza Canyon Formation (Neogene), rather than rhyolitic pumice of the Quaternary El Cajete pumice (Qvec) (c.f. Kempter et al., 2004; see Figure 2 herein). While a seemingly minor issue, it does point to the mixing of obsidian sources in the southern Jemez Mountains and presents another complication for geoarchaeological investigations.

periwinkle gray, light green, purple, tan text in Table 2) compared to other archaeologically relevant rhyolites in the Jemez Mountains: Valles, Cerro Toledo, El Rechuelos, and Canovas Canyon (lower part of Table 2).

Obsidians collected from areas mapped as El Cajete pumice in the Bear Springs Peak Quadrangle, southeast of Paliza Canyon, have a composition compatible with the Bearhead Rhyolite. Comparison of trace element concentrations of these samples indicate overlap with the obsidian from the F04–31 Bearhead Rhyolite dome (Figures 5 and 6) but notable dissimilarity with El Cajete pumice and Banco Bonito, the latter two being notably similar (Table 2). Samples of pumice from these obsidian localities also generally do not chemically match the El Cajete pumice. One obsidian sample had a similar chemistry to the Canovas Canyon Rhyolite

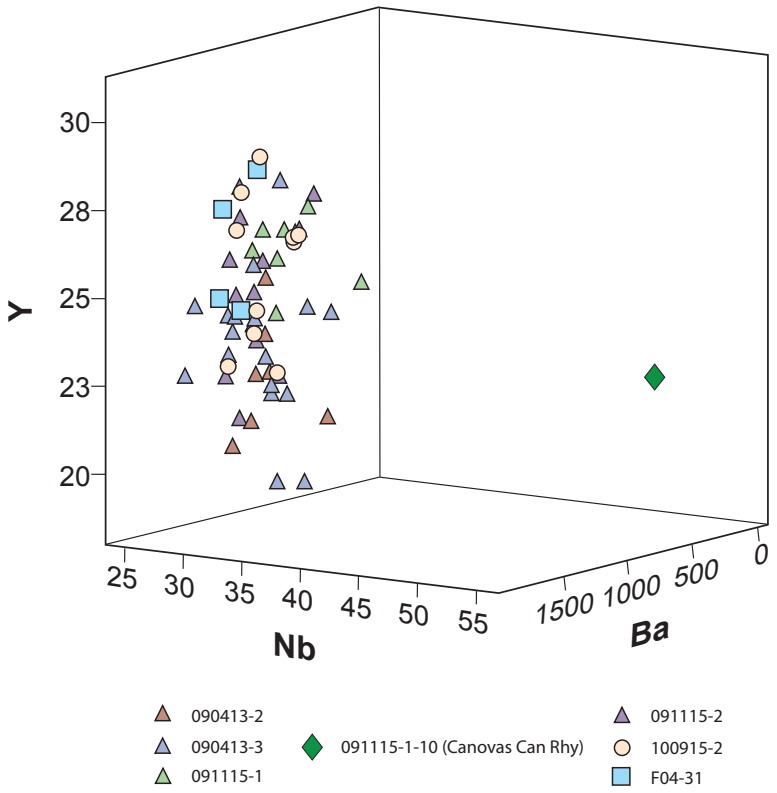

Figure 5. Nb, Y, Ba three-dimensional plot of Bearhead Rhyolite obsidian data in Table 2 and the one Canovas Canyon Rhyolite obsidian marekanite from collection locality 091115–1 (see Fig. 2). Color-coding of collection localities follows that of Table 2.

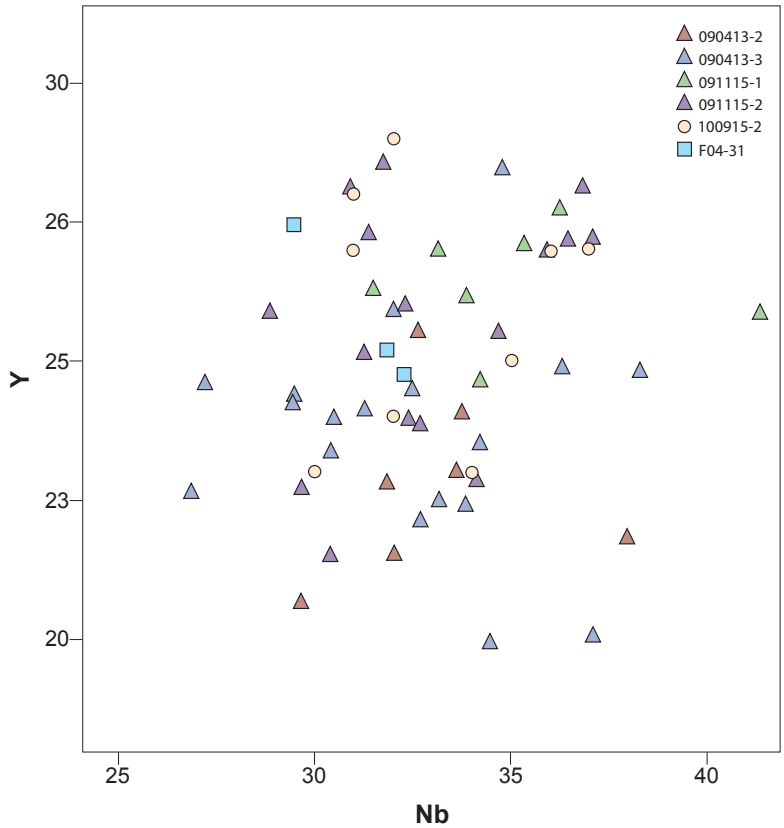

Figure 6. Nb versus Y bivariate plot of Bearhead Rhyolite obsidian data from Table 2. Color-coding of collection localities is from Table 2. Note that the primary source obsidian from the F04–31 Bearhead Rhyolite dome (light blue squares) occupies the same space as secondary deposit samples from Paliza Canyon (100915-2) and collection localities south of Paliza Canyon (see Fig. 2).

TABLE 2. Selected trace element concentrations for obsidian and pumice samples

Sample*	Zn	Rb	Sr	Y	Zr	Nb	Ba	Pb	Th
090413-2-1	81	101	91	23	132	34	1667	19	13
090413-2-2	117	103	89	26	121	33	1611	20	12
090413-2-3	145	87	76	21	112	30	1592	16	14
090413-2-4	124	107	90	23	120	32	1608	20	18
090413-2-5	111	95	79	22	117	32	1664	18	21
090413-2-6	92	99	87	22	126	38	1605	18	14
090413-2-7	92	101	79	24	119	34	1711	19	13
090413-3-1	56	109	94	24	128	34	1741	24	12
090413-3-11	61	100	87	25	121	36	1612	17	17
090413-3-12	58	101	86	22	120	34	1665	19	12
090413-3-14	52	103	86	28	123	35	1685	19	16
090413-3-18	78	105	87	24	122	32	1672	21	12
090413-3-19	101	97	85	23	113	30	1689	18	13
090413-3-2	57	95	85	25	124	38	1607	15	15
090413-3-20	81	102	82	24	120	31	1577	22	10
090413-3-21	87	95	81	23	115	27	1707	17	17
090413-3-23	89	100	85	25	119	27	1656	22	16
090413-3-24	71	93	79	22	128	33	1606	18	10
090413-3-3	47	99	86	26	120	32	1640	23	11
090413-3-4	46	99	86	22	136	33	1445	18	12
090413-3-5	56	105	89	20	138	37	1706	22	19
090413-3-6	47	101	86	20	125	34	1680	19	19
090413-3-7	53	105	93	24	128	29	1560	22	7
090413-3-8	55	102	89	24	134	29	1609	20	13
090413-3-9	47	96	85	24	130	31	1661	22	17
091115-1-1	45	93	85	26	140	41	1651	18	17
091115-1-3	43	100	86	26	130	31	1597	19	8
091115-1-5	56	111	91	26	135	34	1630	23	18
091115-1-6	49	102	86	27	129	35	1699	19	20
091115-1-7	59	98	86	27	132	33	1673	19	14
091115-1-8	54	101	88	25	129	34	1668	20	13
091115-1-9	54	105	89	28	137	36	1601	20	15
091115-1-10 (Canovas Can Rhyolite)	41	116	40	22	104	52	368	26	25
091115-2-1	51	101	89	24	129	33	1679	19	11
091115-2-2	49	99	88	25	125	31	1707	18	17
091115-2-3	52	99	85	21	135	30	1602	22	20
091115-2-4	41	104	85	26	130	29	1542	17	12
091115-2-5	57	108	95	28	136	37	1613	25	12
091115-2-6	55	105	90	26	128	32	1594	21	14
100915-2-1 (“Paliza Canyon” source area)	49	104	90	27	135	36	1661	21	14
100915-2-10 (“Paliza Canyon” source area)	50	95	84	25	127	35	1879	18	10
100915-2-2 (“Paliza Canyon” source area)	54	108	94	27	133	36	1693	19	11
100915-2-3 (“Paliza Canyon” source area)	42	94	80	28	121	31	1642	16	11
100915-2-4 (“Paliza Canyon” source area)	51	105	92	27	140	37	1778	20	14
100915-2-5 (“Paliza Canyon” source area)	45	98	88	24	122	32	1639	20	19
100915-2-6 (“Paliza Canyon” source area)	44	108	93	29	133	32	1593	21	13
100915-2-7 (“Paliza Canyon” source area)	44	99	99	23	128	34	1643	22	14
100915-2-8 (“Paliza Canyon” source area)	41	90	79	23	122	30	1646	16	11
100915-2-9 (“Paliza Canyon” source area)	50	102	94	27	132	31	1686	21	15

Table 2 continued next page.

Table 2 continued from previous page.

Sample*	Zn	Rb	Sr	Y	Zr	Nb	Ba	Pb	Th
F04-31-1 (Bearhead Rhyolite Dome)	45	91	79	25	123	32	1883	15	18
F04-31-2 (Bearhead Rhyolite Dome)	46	104	90	25	142	32	1766	22	16
F04-31-3 (Bearhead Rhyolite Dome)	44	100	85	27	132	29	1655	21	17
Valles Rhyolite (Cerro del Medio)[1]	26[6]	160	10	43	172	54	35	27.7[6]	17.5[6]
Cerro Toledo Rhyolite[1]	n.r.	207	5	63	183	98	23	n.r.	23[4]
El Rechuelos Rhyolite[1]	n.r.	152	9	23	77	47	24	n.r.	16.7[5]
Canovas Canyon Rhyolite[1]	21[3]	116	43	21	108	53	352	n.r.	12.9[7]
El Cajete pumice[8]	32[2]	136	185	27	125	36	616	19	18
Banco Bonito Rhyolite obsidian[8]	30[3]	143	192	28	136	39	596	20	18.6
RGM-1 (this study)	39	151	104	27	218	8	806	24	18
RGM-1 USGS recommended	32	150	110	25	220	8.9	810	24	15

*39 Bearhead Rhyolite obsidian samples were collected from areas previously mapped as El Cajete pumice (brown, periwinkle gray, light green, and purple text for 090413-2-n, 090413-3-n, 091115-1-n, and 091115-2-n respectively), 10 samples of alluvial obsidian from the "Paliza Canyon" source area (tan text), and 3 samples of obsidian from the F04-31 Bearhead Rhyolite dome (light blue text; Goff et al., 2006). Comparative samples include: El Cajete pumice, one sample each from known artifact quality obsidian sources from the Jemez Mountains, and the USGS RGM-1 rhyolite standard (see Shackley 2005). Note that color-coded localities correspond with colors plotted in elemental plots (Figures 5 and 6).
[1] Mean concentrations mainly from unit Qvdmw of Gardner et al. (2007); see Appendix in Shackley 2005.
[2] Zn concentration from F. Goff, unpub. data.
[3] Zn concentration from Gardner et al. (1986).
[4] Th concentration from Stix et al. (1988).
[5] Th concentration from Loeffler et al. (1988).
[6] Zn, Pb and Th concentrations from Gardner et al. (2007); obsidian unit Qvdmw.
[7] Th concentration from Gardner et al. (1986).
[8] Except for Zn, the El Cajete pumice and Banco Bonito obsidian values are from Self et al. (1988).
n.r. = not reported.

TABLE 3. Mean and central tendency for Bearhead Rhyolite obsidian from data in Table 2 and mean data from the four "Paliza Canyon" samples originally reported by Baugh and Nelson (1987).

Element	N	Minimum	Maximum	Mean[1]	σ
Zn	61	41	145	60 (n.r.)[2]	22.5
Rb	61	87	111	100 (100.8)	5.3
Sr	61	76	99	87 (86.2)	5.1
Y	61	20	29	25 (8.5)	2.2
Zr	61	112	142	128 (124)	7.1
Nb	61	27	41	33 (18.1)	2.8
Ba	61	1445	1883	1660 (1352)	75.1
Pb	61	15	25	20 (n.r.)	2.1
Th	61	7	21	14 (n.r.)	3.1

[1] Baugh and Nelson (1987) mean values reported in parentheses.
[2] n.r. = not reported by Baugh and Nelson (1987).

(sample 091115–1–10; Table 2, Fig. 5). The remaining tephra samples were dacitic (091115–2–7, 091115–2–8, and 091115–2–9 samples in Table 1 and Fig. 4) and likely part of the Paliza Canyon Formation, as discussed below.

Discussion

Sources for the formally known "Paliza Canyon" obsidian

The geochemistry in the preceding section demonstrates that the "Paliza Canyon obsidian" in the archaeological vernacular compares very well with Bearhead Rhyolite obsidian, consistent with geologic relations near the obsidian source locality of Nelson (1984) and Baugh and Nelson (1987). We interpret that the primary sources of this obsidian are domes of Bearhead Rhyolite near the head of Paliza Canyon in the southern Jemez Mountains, one of which is the F04–31 dome of Goff et al., (2006). Small but fresh obsidian fragments (marekanites or Apache tears) are also associated with the Peralta Tuff Member of the Bearhead Rhyolite (ca. 7 Ma) in the southeastern Jemez Mountains (F. Goff, unpublished data). Whether the Peralta Tuff material is artifact quality obsidian from an unknown locale is not yet clear. Other geologic source areas near Paliza Canyon are discredited for reasons enumerated below.

Geologists working in the Jemez Mountains have noted that obsidian is abundant in the upper part of the El Cajete pumice that outcrops near all the collection localities (references above, especially Goff et al., 2006; Kempter et al., 2004). In fact, we initially hypothesized that the El Cajete pumice was the source of what we now call Bearhead Rhyolite obsidian. However, the obsidians from the sampled tephras southeast of Paliza Canyon in the Bear Springs Peak Quadrangle chemically match the Bearhead Rhyolite, as noted above. Furthermore,

the associated tephra are dacitic in composition, based on hand lens examination plus major and minor oxide chemistry data (Table 1; TAS plot in Fig. 4). The dacitic tephras are probably from dome eruptions associated with the Paliza Canyon Formation, such as unit Tpbhd to the north (Fig. 2), or pumice from various Paliza Canyon Formation domes reworked into volcaniclastic gravels (Tpv) of the Keres Group (see Goff et al., 2006; Kempter et al., 2004). These older Keres Group tephras and gravels appear to be overlain by a thin and discontinuous cover of El Cajete pumice, at least in our sampled area above and southeast of Paliza Canyon. For example, tephra and reworked obsidian from unit Tpv underlies a very thin blanket of El Cajete pumice at sampling locality 091115–1.

Another possible source is the Canovas Canyon Formation, which locally has obsidian. However, Canovas Canyon Formation obsidian is readily differentiated from Bearhead Rhyolite obsidian by their lower Sr and Ba concentrations and, to a lesser extent, differences in Y and Nb composition (Table 2; Fig. 5). One of marekanite samples from collection locality 090413–3/091115–1 (same locality, two separate collection dates), in what we thought was El Cajete pumice, had similar chemistry to the Canovas Canyon Formation (Table 2, sample 091115-1-10)–although all the other collected obsidian at this locality was Bearhead Rhyolite obsidian (Fig. 5). Like the aforementioned Paliza Canyon dacitic tephras, the marekanite represented by sample 091115-1-10 is interpreted to have been reworked into the Keres Group from a Canovas Canyon Formation source. The Canovas Canyon Rhyolite is mapped just southeast of our study area, so this is not unexpected (see Fig. 2 and Kempter et al., 2004).

Despite their aforementioned geochemical differences, the Bearhead Rhyolite obsidian and Canovas Canyon Rhyolite obsidian are characterized by the highest Sr and Ba and lowest Rb of all the Jemez Mountain sources (Table 2), indeed all the archaeological obsidian from Jemez Lineament obsidian sources (Mount Taylor and Jemez Mountains in Shackley 2005). Both Bearhead Rhyolite obsidian (ca. 7 Ma) and Canovas Canyon Rhyolite (Bear Springs Peak) obsidian (ca. 8.85–9.7 Ma) have been eroding down into the Rio Grande for millions of years (Goff et al., 2006; Kempter et al. 2004). While representing relatively small percentages of obsidian provenance assemblages in North American Southwestern archaeological sites, they nevertheless are geochemically different than the more common Jemez Mountains obsidian sources such as Cerro Toledo Rhyolite, El Rechuelos Rhyolite, and Valles Rhyolite (Cerro del Medio).

Archeological Implications

The largest Bearhead Rhyolite marekanite recovered was 100 mm in largest dimension but most were 10–30 mm, with a few 30–40 mm. Given that recycled Bearhead Rhyolite obsidian recovered at Tijeras Wash (south of Albuquerque, more than 150 stream km south of the southern Jemez Mountains) are as much as 3 mm in largest dimension, obsidian from the primary sources must have been significantly larger than the marekanites recovered in this study. In October 2015, we recovered a marekanite nearly 100 mm in diameter (sample 100915-2-1 in Table 2 and Fig. 3) in alluvium filling Paliza Canyon just downstream from the F04–31 Bearhead Rhyolite dome, certainly large enough to supply samples downstream through fluvial transport along the Rio Grande. As a media for tool production, this smoky gray to nearly transparent obsidian is equal in quality to other Jemez Mountains sources, as the Ancestral Puebloans found during the Pueblo Revolt period.

Pueblo Revolt period knappers in the area used this obsidian due to proximity, but it was also used as a raw material throughout prehistory in the region (Shackley 2014a, 2014b, 2015; see below). Other than archaeological contexts in the immediate Jemez Mountains region, one could argue that this Bearhead Rhyolite obsidian is a minor component of archaeological obsidian raw material used in the Southwest. These "minor" sources do have potential to illuminate past human behavior and can be as important as major sources, as has been argued elsewhere (Shackley 2009b, 2009c). A recent example from northern New Mexico proves illuminating.

At the Late Archaic Early Agricultural site of San Luis de Cabezón northwest of Cuba, New Mexico (LA 110946), the obsidian assemblage was dominated by artifacts, mainly debitage (waste flakes) produced from Cerro Toledo Rhyolite (64.4%) and Valles Rhyolite (Cerro del Medio; 25%), the sources of which are about a day's walk away in the Jemez Mountains to the east (n=104 obsidian artifacts; Shackley 2014b). What is notable is that many of the

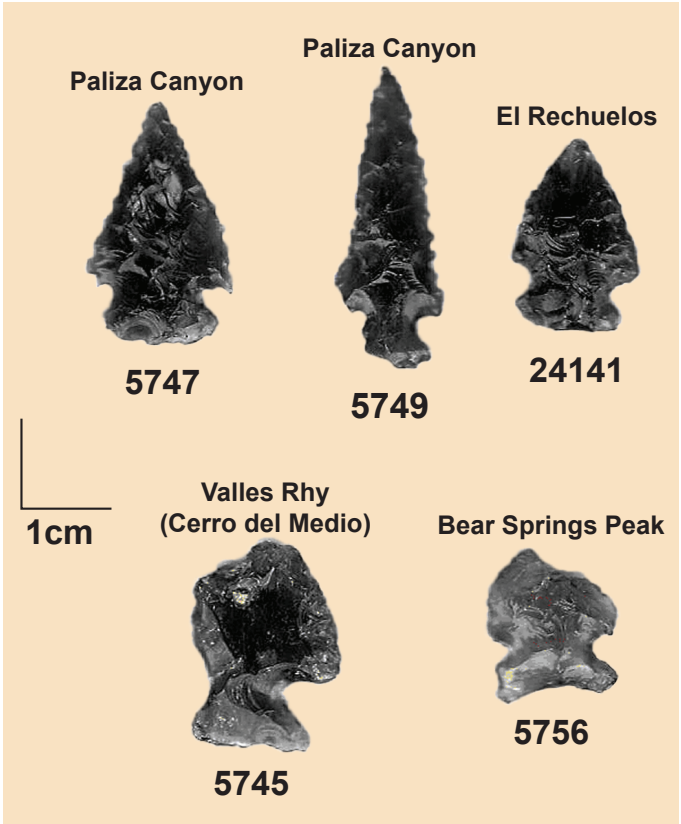

Figure 7. Late Archaic obsidian projectile points and source provenance from San Luis de Cabezón (LA 110946) produced from Bearhead Rhyolite (previously called Paliza Canyon) and Canovas Canyon Rhyolite (Bear Springs Peak) obsidian, and one produced from Valles Rhyolite and El Rechuelos Rhyolite obsidian (from Shackley 2014b). Projectile point 5749 is nearly 35 mm in length produced from a Bearhead Rhyolite obsidian core at least 40 mm in diameter. Note: spherulite in sample 5745 typical of Cerro del Medio obsidian and generally not present in the Keres Group obsidians.

obsidian projectile points recovered (Fig. 7) were produced from Keres Group sources that are in the southern portion of the Jemez Mountains and nearer to this site. These Keres Group sources include Bearhead Rhyolite (previously called "Paliza Canyon"; 4.8% of total obsidian), Canovas Canyon Rhyolite (3.8% of total obsidian), the only artifact produced from Polvadera Group El Rechuelos on the north side of Valles Caldera, and one projectile point produced from Tewa Group Valles Rhyolite, although Valles Rhyolite debitage comprised 25% of the overall assemblage (Fig. 7; Shackley 2014b). The Keres Group sources are small Neogene marekanite sources, but provide excellent media for flaked stone tool production and are located nearer to the Cabezón site than most of the other Jemez sources. Additionally, projectile points produced from Bearhead Rhyolite obsidian at San Luis de Cabezón were near 50 mm in length, and so had to be produced from cores larger than 50 mm in size–within the range of marekanites recovered in Paliza Canyon just below the F04-31 dome.

The above discussion suggests that the raw material at San Luis de Cabezón was procured from the primary dome or nearby in the southern Jemez Mountains rather than from secondary deposits to the south. Therefore, the presence of "minor" obsidian sources in this case elucidates prehistoric hunting and raw material procurement behavior that might not be obvious looking at the major sources in the Jemez Mountains alone. Indeed, understanding the primary location of a raw material source is crucial in more precisely defining behavior, even if the source is a "minor" source.

The unity of geology and archaeology, a long–standing relationship, can offer clarity to both disciplines. An entire Geological Society of America volume was devoted to this relationship (Stein and Linse 1993). The Bearhead Rhyolite obsidian project is a prime example of this "symbiotic" relationship, and in part shows the differences in scientific scale between these closely related disciplines. Our discovery of dacitic tephra (reworked from the Paliza Canyon Formation) in what has previously been mapped as El Cajete Rhyolite is mainly due to a finer-grained approach common in archaeology. Mapping with this finer-grained approach, particularly in archaeological sites, is often required to be at the millimeter level, a scale rare in geological mapping. This archaeological perspective is often brought into geoarchaeological investigations and, as seen here, has ramifications for geological interpretation.

Acknowledgements

We dedicate this paper to the late Dr. Jamie Gardner, a friend and colleague who was always helpful to both Goff and Shackley and one of the pivotal geologists in Jemez Mountains research. The field research was carried out under Santa Fe National Forest Permit SFE222401 to Shackley. We thank Mike Bremer of the Santa Fe National Forest for continual support of geoarchaeological obsidian provenance research on the forest. We also thank Leo Gabaldon of the NMBGMR (New Mexico Bureau of Geology and Mineral Resources) for drafting of Figure 2 and finalizing the other figures. Dan Koning (NMBGMR) ably handled the editorial chores. Kathy Butler helped during fieldwork of the initial reconnaissance in 2013. Tim Baugh pointed us to the general area in Paliza Canyon where the four obsidian "source" samples were originally recovered--and what began this journey. Finally, we thank Nelia Dunbar (NMBGMR) and Gary Smith (University of New Mexico) for scientific editing that substantially improved the draft manuscript.

References

Baugh, T.G., and Nelson, F.W., Jr., 1987, New Mexico obsidian sources and exchange on the Southern Plains: Journal of Field Archaeology, v.14, p. 313–329.

Church, T., 2000, Distribution and sources of obsidian in the Rio Grande gravels of New Mexico: Geoarchaeology, v. 15, p. 649–678.

Ellisor, R., Wolff, J. & Gardner, J.N., 1996, Outline of the petrology and geochemistry of the Keres Group lavas and tuffs, in Goff, F., Kues, B.S., Rogers, M.A., McFadden, L.D., and Gardner, J.N., eds., The Jemez Mountains Region: New Mexico Geological Society, 47th Annual Field Conference, Guidebook, p. 237–242.

Gardner, J.N., Goff, F., Garcia, S., and Hagan, R.C., 1986, Stratigraphic relations and lithologic variations in the Jemez Volcanic Field, New Mexico: Journal of Geophysical Research, v. 91, B2, p. 1763–1778.

Gardner, J.N., Sandoval, M.M., Goff, F., Phillips, E., and Dickens, A., 2007, Geology of the Cerro Del Medio moat rhyolite center, Valles caldera, New Mexico, in Kues, B.S., Kelley, S.A., and Lueth, V.W., eds., Geology of the Jemez Region II: New Mexico Geological Society, 58th Annual Field Conference, Guidebook, p. 367–372.

Gardner, J.N., Goff, F., Kelley, S., and Jacobs, E., 2010, Rhyolites and associated deposits of the Valles–Toledo caldera complex: New Mexico Geology, v 32, p. 3–18.

Glascock, M.D., Kunselman, R., and Wolfman, D., 1999, Intrasource chemical differentiation of obsidian in the Jemez Mountains and Taos Plateau, New Mexico: Journal of Archaeological Science, v. 26, p. 861–868.

Goff, F., and Gardner, J.N., 2004, Late Cenozoic geochronology of volcanism and mineralization in the Jemez Mountains and Valles caldera, north central New Mexico, *in* Mack, G. and Giles, K., eds., The Geology of New Mexico —A Geologic History: New Mexico Geological Society, Special Publication 11, p. 295–312.

Goff, F., Kues, B.S., Rogers, M.A., McFadden, L.D., and Gardner, J.N., eds., 1996, The Jemez Mountains region: New Mexico Geological Society, 47th Annual Field Conference, Guidebook, 484 p.

Goff, F., Gardner, J.N., Reneau, S.L., and Goff, C.J., 2006, Geology of the Redondo Peak 7.5 minute quadrangle, Sandoval County, New Mexico: New Mexico Bureau of Geology and Mineral Resources Open-File Geologic Map OF–GM 111, scale 1:24,000.

Goff, F., Gardner, J.N., Reneau, S.L., Kelley, S.A., Kempter, K.A., and Lawrence, J.R., 2011, Geologic map of the Valles caldera, Jemez Mountains, New Mexico: New Mexico Bureau of Geology and Mineral Resources, Geologic Map 79, scale 1:50,000.

Justet, L., 1996, The geochronology and geochemistry of the Bearhead Rhyolite, Jemez volcanic field, New Mexico [Master's thesis]: Las Vegas, University of Nevada, 152 p.

Justet, L., 2003, Effects of basalt intrusion on the multi-phase evolution of the Jemez volcanic field, New Mexico [Ph.D. thesis], Las Vegas, University of Nevada, 248 p.

Lajčáková, A. and Kraus, I., 1993, Volcanic glasses, in Bouška, V., ed., Natural Glasses: New York, Ellis Horwood, p. 85–121.

Kelley, S.A., McIntosh, W.C., Goff, F., Kempter, K.A., Wolff, J.A., Esser, R., Braschayko, S., Love, D., and Gardner, J.N., 2013, Spatial and temporal trends in pre-caldera Jemez Mountains volcanic and fault activity: Geosphere, v. 9, p. 614–646.

Kempter, K., Osburn, G.R., Kelley, S.A., Rampey, M., Ferguson, C., and Gardner, J.N., 2004, Preliminary geologic map of the Bear Springs Peak quadrangle, Sandoval County, New Mexico: New Mexico Bureau of Geology and Mineral Resources Open-File Geologic Map OF–GM 74, scale 1:24,000.

Kues, B.S., Kelley, S.A., and Lueth, V.W., 2007, Geology of the Jemez Region II: New Mexico Geological Society, 58th Annual Field Conference, Guidebook, 499 p.

Le Bas, M.J., Le Maitre, R.W., Streckeisen, A., and Zanettin, B., 1986, A chemical classification of volcanic rocks based on the total alkali-silica diagram: Journal of Petrology, v. 27, p. 745–750.

Liebmann, M., 2012, Revolt: An archaeological history of pueblo resistance and revitalization in the 17th century New Mexico: Tucson, University of Arizona Press, 328 p.

Loeffler, B.M., Vaniman, D.T., Baldridge, W.S., and Shafiqullah, M., 1988, Neogene rhyolites of the northern Jemez volcanic field, New Mexico: Journal of Geophysical Research, v. 93, p. 6157–6167.

Nelson, F.W., Jr., 1984, X-ray fluorescence of some western North American obsidians, in Hughes, R.E., ed., Obsidian Studies in the Great Basin: Berkely, University of California, Contributions of the University of California Archaeological Research Facility 45, p. 27–62.

Phillips, E.H., Goff, F., Kyle, P.R., McIntosh, W.C., Dunbar, N.W., and Gardner, J.N., 2007, The $^{40}Ar/^{39}Ar$ age constraints on the duration of resurgence at the Valles caldera, New Mexico: Journal of Geophysical Research, v.112, B08201, 15 p.

Self, S., Goff, F., Gardner, J.N, Wright, J.V., and Kite, W.M., 1986, Explosive rhyolitic volcanism in the Jemez Mountains: vent locations, caldera development, and relation to regional structure: Journal of Geophysical Research, v. 91, B2, p. 1779–1798.

Self, S., Kirchner, D.E., and Wolff, J.A., 1988, The El Cajete Series, Valles Caldera, New Mexico: Journal of Geophysical Research, v. 93, B6, p. 6113–6127.

Shackley, M.S., 2005, Obsidian: geology and archaeology in the North American Southwest: Tucson, University of Arizona Press, 264 p.

Shackley, M.S., 2009a, Source provenance of obsidian artifacts from six ancestral pueblo villages in and around the Jemez Valley, Northern New Mexico: unpublished report prepared for Matthew Liebmann, Department of Anthropology, Harvard University, 17 p.

Shackley, M.S., 2009b, Two newly discovered sources of archaeological obsidian in the Southwest: archaeological and social implications: Kiva v. 74, p. 269–280.

Shackley, M.S., 2009c, The Topaz Basin archaeological obsidian source in the Transition Zone of central Arizona: Geoarchaeology, v. 24, p. 336–347.

Shackley, M.S., 2011, An introduction to X-ray fluorescence (XRF) analysis in archaeology, *in* Shackley, M.S., ed., X-Ray Fluorescence Spectrometry (XRF) in Geoarchaeology: New York, Springer Publishing, p. 7–44.

Shackley, M.S., 2012a, The secondary distribution of archaeological obsidian in Rio Grande Quaternary sediments, Jemez Mountains to San Antonito, New Mexico: inferences for prehistoric procurement and the age of sediments: Poster presentation at the Society for American Archaeology, annual meeting, Memphis, Tennessee.

Shackley, M.S., 2012b, Source provenance of obsidian artifacts from Astialakwa (LA 1825) Jemez Valley, New Mexico: unpublished report prepared for Matthew Liebmann, Department of Anthropology, Harvard University, 11 p.

Shackley, M.S., 2014a, Source provenance of obsidian artifacts from The El Segundo archaeology project, Northwestern New Mexico: unpublished report prepared for Southwest Archaeological Consultants, Santa Fe, New Mexico, 43 p.

Shackley, M.S., 2014b, Source provenance of obsidian artifacts from 17 archaeological sites along the MAPL WEPIII project alignment, northwestern to southeastern New Mexico: unpublished report prepared for the Office of Contract Archeology, University of New Mexico, Albuquerque, 30 p.

Shackley, M.S., 2015, Source provenance of obsidian artifacts from The El Segundo archaeology project, Northwestern New Mexico: unpublished report prepared for Southwest Archaeological Consultants, Santa Fe, New Mexico, 72 p.

Spell, T.L., and Harrison, T.M., 1993, $^{40}Ar/^{39}Ar$ geochronology of post-Valles Caldera rhyolites, Jemez Volcanic Field, New Mexico: Journal of Geophysical Research v. 98, B5, p. 8031–8051.

Stein, J.K., and Linse, A.R., eds. 1993, Effects of Scale on Archaeological and Geoscientific Perspectives: Boulder Colorado, Geological Society of America Special Paper 283, 91 p.

Stix, J., Goff, F., Gorton, M.P., Heiken, G., and Garcia, S.R., 1988, Restoration of compositional zonation in the Bandelier silicic magma chamber between two caldera-forming eruptions: Geochemistry and origin of the Cerro Toledo Rhyolite, Jemez Mountains, New Mexico: Journal of Geophysical Research, v. 93, p. 6129–6147.

Wolfman, D., 1994, Jemez Mountains chronology study: Santa Fe, Museum of New Mexico, Office of Archaeological Studies, 234 p.: **http://members.peak.org/~obsidian/pdf/wolfman_1995.pdf** (accessed September 2016).

Zimmerer, M.J., Lafferty, J., and Coble, M.A., 2016, The eruptive and magmatic history of the youngest pulse of volcanism at the Valles caldera: Implications for successfully dating late Quaternary eruptions: Journal of Volcanology and Geothermal Research, v. 310, p. 50–57.

Appendix

The ThermoFisher/Scientific QUANT'X EDXRF Spectrometer methods at the Geological XRF Laboratory

This appendix presents analytical methodology for the EDXRF Spectrometer used in this study (modified slightly from **http://swxrflab.net/anlysis.htm**). All archaeological samples are analyzed whole. The results presented here are quantitative in that they are derived from "filtered" intensity values ratioed to the appropriate x-ray continuum regions through a least squares fitting formula rather than plotting the proportions of the net intensities in a ternary system (McCarthy and Schamber 1981; Schamber 1977). Or more essentially, these data, through the analysis of international rock standards, allow for inter-instrument comparison with a predictable degree of certainty (Hampel 1984).

The spectrometer is equipped with: (1) a peltier air cooled solid-state Si(Li) X-ray detector having an ultra ultra-high-flux end window bremsstrahlung rhodium (Rh) x-ray target with a 125 micron beryllium (Be) window and an 8.8 mm collimator (3.5 mm for samples < 10mm diameter), and (2) x-ray generator that operates from 4–50 kV/0.02–1.0 mA at 0.02 increments using an IBM PC based microprocessor and WinTraceTM 7.0 software. The spectrometer is equipped with a 2001 min-1 Edwards vacuum pump for the analysis of elements below titanium (Ti). Data is acquired with a pulse processor and analog to digital converter. This is a significant improvement in analytical speed and efficiency beyond the former Spectrace 5000 and QuanX analog systems (see Davis et al., 2011; Shackley 2005).

Trace Element Analyses

For Ti-Nb, Pb, Th elements the mid-Z(b) group condition is used operating the x-ray tube at 30 kV. The x-ray tube utilizes a 0.05 mm (medium) Pd primary beam filter in an air path at 200 seconds livetime to generate x-ray intensity Kα1-line data for elements titanium (Ti), manganese (Mn), iron (as FeT), cobalt (Co), nickel (Ni), copper (Cu), zinc (Zn), gallium (Ga), rubidium (Rb), strontium (Sr), yttrium (Y), zirconium (Zr), niobium (Nb), lead (Pb), and thorium (Th). Not all these elements are reported since their values in many volcanic rocks are very low and below detection limits. Trace element intensities were converted to concentration estimates by employing a least-squares or quadratic calibration line ratioed to the Compton scatter established for each element from the analysis of international rock standards certified by the National Institute of Standards and Technology (NIST), the US. Geological Survey (USGS), Canadian Centre for Mineral and Energy Technology, and the Centre de Recherches Pétrographiques et Géochimiques in France (Govindaraju 1994). Line fitting is linear (XML) for all elements. When barium (Ba) data are acquired, the Rh tube is operated at 50 kV and .25–1.0 mA (automated) in an air path at 200 seconds livetime to generate x-ray intensity Kα1-line data, through a 0.630 mm Cu (thick) filter ratioed to a portion of the bremsstrahlung region (see Davis et al., 2011). Further details concerning the petrological choice of these elements in Southwest obsidians is available in Shackley (2005; also Mahood and Stimac 1991; and Hughes and Smith 1993). A suite of 16 specific U.S. Geological Survey standards are used for the best fit regression calibration for elements Ti- Nb, Ba, Pb, and Th: G-2 (basalt), AGV-2 (andesite), GSP-2 (granodiorite), SY-2 (syenite), BHVO-2 (hawaiite), STM-1 (syenite), QLO-1 (quartz latite), RGM-1 (obsidian), W-2 (diabase), BIR-1 (basalt), SDC-1 (mica schist), BCR-2 (basalt), TLM-1 (tonalite), SCO-1 (shale), NOD-A-1 (manganese), NOD-P-1 (manganese). Four other standards include: National Institute of Standards and Technology NIST-278 (obsidian), BR-E (basalt) from the Centre de Recherches Pétrographiques et Géochimiques in France, and JR-1 and JR-2 (obsidian) from the Geological Survey of Japan (Govindaraju 1994).

The data from the WinTrace software are translated directly into Excel for Windows software for manipulation and into SPSS for Windows for statistical analyses when necessary.

TABLE 1. X-ray fluorescence concentrations for selected trace elements from obsidian standard RGM-1*

SAMPLE	Ti	Mn	Fe	Rb	Sr	Y	Zr	Nb	Ba	Pb	Th
RGM-1											
(Govindaraju 1994)	1600[1]	279	12998	149	108	25	219	8.9	807	24	15.1
RGM-1 (USGS recommended)[1]	1618±120	279±50	12998±210	150±8	110±10	25[2]	220±20	8.9±0.6	810±46	24±3	15±1.3
GeoRem values[2]	1510–1940	282	12788–14263	142–164	96.73–116	21.6–25.1	173–258	8.37–13	791–881	18–28.4	14–16.3
RGM-1, pressed powder (this study, n=99)	1523±49	294±13	13723±30	149±2	108±2	25±2	219±2	9±2.0	804[3]	21±1.6	17±3.2
RGM-1, flake from original USGS boulder (n=12)	1568±44	311±11	13306±33	153±2	113±2	25±1.5	230±4	9±2	942±14	23±1.5	15±3.4

* Pressed powder and whole rock elemental analysis of USGS RGM-1 obsidian standard measured on the ThermoScientific Quant'X, which are compared to USGS, Govindaraju (1994), and GeoRem recommended values. USGS RGM-1 pressed powder pellet (n=99 runs) and whole rock flake are from original USGS boulder (n=12). ± values represent first standard deviation computations for the group of measurements. All values are in parts per million (ppm) as reported in Govindaraju (1994), USGS, and this study. RGM-1 is a U.S. Geological Survey obsidian standard obtained from Glass Mountain, Medicine Lake Highlands Volcanic Field, northern California.

[1] Ti, Mn, Fe calculated to ppm from wt. percent from USGS data using MURR's oxide to element and element to oxide multiplier table (from Glascock 1991): **http://swxrflab.net/MURRoxidetoelementtable.jpg**

[2] information value

[3] n=17

In order to evaluate these quantitative determinations, machine data were compared to measurements of known standards during each run (Table 1). RGM-1 is analyzed during each sample run (n=1–19) for obsidian artifacts to check machine calibration. Other appropriate standards from the above list are used for other volcanic rocks.

Detection limits

Detection limits for EDXRF have been calculated at 6 Σ at this web site: **http://swxrflab.net/detectionlimits.htm**. Recently, a number of scholars have questioned the validity of using pressed powder pellets of international standards for empirical calibration and data checking. This concern, called a "matrix issue," questions the potential differing analytical results between pressed powder and whole rock samples (Jeff Ferguson, personal communication, 2010; cf. Shackley 2011). The potential problem was tested in detail in Kathleen Davis et. al.'s, (1998, reprinted 2011) study of EDXRF on obsidian and found to not be an issue (see also Shackley and Hampel 1992). Hermes and Ritchie (1997) derived similar conclusions using EDXRF with archaeological felsites. Table 1 exhibits the analysis of one of my pressed powder pellets of USGS RGM-1 and a flake from the same USGS collected boulder sent by Steve Wilson of the USGS. As one can see, the variability is within 1% or less in most cases, and some of this variability is inherent in the native variability within the single 200 kg boulder collected at Glass Mountain by USGS, not because of differing matrices. This issue is well examined by Ron Jenkins and seems to be misunderstood in the discipline (c.f. Jenkins 1999:167–172). While it is true that his discussion hinges on the assumption of homogeneity, one must assume that for purposes of non-destructive EDXRF that pressed powder standards are heterogeneous while obsidian is homogeneous. This is, indeed, not the case for obsidian studies in general. Jenkins explains:

> "Primary absorption occurs because all atoms of the specimen matrix will absorb photons from the primary source. Since there is a competition for these primary photons by the atoms making up the specimen [pressed powder versus glass], the intensity/wavelength distribution of these photons available for the excitation of a given analyte element may be modified by other matrix effects (Jenkins 1999:168; emphasis mine)."

In the case of pressed powder pellets, the "competition" involves air molecules locked in the powder matrix, which is not analyzed in obsidian studies and of course is not present in volcanic glass, particularly with XRF and ICP-MS technology. While it is true that the borate mix used in the pressed powder can yield some boron, this element is undetectable by XRF and so light (Z=5) as to not cause peak overlap, especially when using any tube filtering. Perhaps more important is the issue of infinite thickness, particularly when Z≥51 and high tube voltages are required. In this case, some of the x-rays are radiated through the sample, and ratioing to the Compton or bremsstrahlung regions can yield complex results, as can be seen in Table 1 for Ba and evidently a problem for other analysts as well, as seen by the GeoRem values in Table 1. In this case, careful calibration can mitigate some of this error. Parenthetically, only recently have PXRF products been able to reach 50 kV in order to adequately move electrons out of orbit for those atoms Z≥51, despite opinion to the contrary (see Jenkins 1999:9–12; Speakman and Shackley 2013).

As I've noted in print and in discussions with many of my colleagues, not using international standards, as is often seen in PXRF studies, severely hinders the potential for establishing validity in obsidian research. Unless international standards are used, it is nearly impossible to compare results across laboratories (Shackley 2010, 2011; Speakman and Shackley 2013). Therefore, using the "matrix" issue as an excuse is unacceptable.

Major Oxide Analyses

Analysis of the major oxides of Si, Al, Ca, Fe, K, Mg, Mn, Na, and Ti is performed under the multiple conditions elucidated in Table 2. This fundamental parameter analysis (theoretical with standards), while not as accurate as destructive analyses (pressed powder and fusion disks), is usually within a few percent of actual based on the analysis of USGS RGM-1 obsidian standard (see also Shackley 2011). The fundamental parameters (theoretical) method is run under conditions commensurate with the elements of interest and calibrated with 11 USGS standards (RGM-1, rhyolite; AGV-2, andesite; BHVO-1, hawaiite; BIR-1, basalt; G-2, granite; GSP-2, granodiorite; BCR-2, basalt; W-2, diabase; QLO-1, quartz latite; STM-1, syenite), and one Japanese Geological Survey rhyolite standard (JR-1). See Lundblad et al., (2011) for an alternative set of conditions and methods for oxide analyses.

TABLE 2. Conditions of Fundamental Parameter Analysis[1]

Low Za (Na, Mg, Al, Si, P)			
Voltage	6 kV	Current	Auto[2]
Livetime	100 seconds	Counts Limit	0
Filter	No Filter	Atmosphere	Vacuum
Maximum Energy	10 keV	Count Rate	Low
Mid Zb (K, Ca, Ti, V, Cr, Mn, Fe)			
Voltage	32 kV	Current	Auto
Livetime	100 seconds	Counts Limit	0
Filter	Pd (0.06 mm)	Atmosphere	Vacuum
Maximum Energy	40 keV	Count Rate	Medium
High Zb (Sn, Sb, Ba, Ag, Cd)			
Voltage	50 kV	Current	Auto
Livetime	100 seconds	Counts Limit	0
Filter	Cu (0.559 mm)	Atmosphere	Vacuum
Maximum Energy	40 keV	Count Rate	High
Low Zb (S, Cl, K, Ca)			
Voltage	8 kV	Current	Auto
Livetime	100 seconds	Counts Limit	0
Filter	Cellulose (0.06 mm)	Atmosphere	Vacuum
Maximum Energy	10 keV	Count Rate	Low

[1] Multiple conditions designed to ameliorate peak overlap identified with digital filter background removal, least squares empirical peak deconvolution, gross peak intensities and net peak intensities above background.
[2] Current is set automatically based on the mass absorption coefficient.

References

Davis, M.K., Jackson, T.L., Shackley, M.S., Teague, T., and Hampel J., [new introduction by M.S. Shackley], 2011, Factors affecting the energy-dispersive x-ray fluorescence (EDXRF) analysis of archaeological obsidian, in Shackley, M.S., ed., X-Ray Fluorescence Spectrometry (XRF) in Geoarchaeology: New York, Springer Publishing, p. 45–64.

Glascock, M.D., 1991, Tables for neutron activation analysis (3rd edition): University of Missouri, Columbia, Research Reactor Facility.

Govindaraju, K., 1994, Compilation of working values and sample description for 383 geostandards: Geostandards Newsletter v. 18 (special issue), 158 p.

Hampel, J.H., 1984, Technical considerations in x-ray fluorescence analysis of obsidian; in R.E. Hughes ed., Obsidian Studies in the Great Basin: Berkeley, Contributions of the University of California Archaeological Research Facility v. 45, p. 21–25.

Hermes, O.D., and Ritchie, D., 1997, Nondestructive trace element analysis of archaeological felsite by energy-dispersive x-ray fluorescence spectroscopy: Geoarchaeology, v. 12, p. 31–40.

Jenkins, R., 1999, X-Ray Fluorescence Spectrometry (2nd edition): New York, Wiley-Interscience, 207 p.

Lundblad, S.P., Mills, P.R., Drake-Raue, A., and Kikiloi, S.K., 2011, Non-destructive EDXRF Analyses of Archaeological Basalts, *in* M.S. Shackley, ed., X-Ray Fluorescence Spectrometry (XRF) in Geoarchaeology: New York, Springer Publishing, p. 65–80.

McCarthy, J.J., and Schamber, F.H., 1981, Least-squares fit with digital filter: a status report, *in* K.F.J. Heinrich, Newbury, D.E., Myklebust, R.L., and Fiori, C.E., eds., Energy Dispersive X-ray Spectrometry: Washington, D.C., National Bureau of Standards Special Publication 604, p. 273–296.

Schamber, F.H., 1977, A Modification of the linear least-squares fitting method which provides continuum suppression, *in* T.G. Dzubay, ed. X-ray Fluorescence Analysis of Environmental Samples: Ann Arbor Science Publishers, p. 241–257.

Shackley, M.S., 2005, Obsidian: geology and archaeology in the North American Southwest: Tucson, University of Arizona Press, 246 p.

Shackley, M.S., 2010, Is there reliability and validity in portable x-ray fluorescence spectrometry (PXRF)?: The SAA Archaeological Record, Nov. 2010, p. 17–18 and 20.

Shackley, M.S., 2011, Glossary, *in* M.S. Shackley, ed., X-Ray Fluorescence Spectrometry (XRF) in Geoarchaeology: New York, Springer Publishing, p. 207–226.

Shackley, M.S. and Hampel, J., 1992, Surface effects in the energy-dispersive X-ray fluorescence (EDXRF) analysis of archaeological obsidian: 28th International Symposium on Archaeometry, Los Angeles.

Speakman, R.J., and Shackley, M.S., 2013, Silo science and portable XRF in archaeology: a response to Frahm: Journal of Archaeological Science, v. 40, p. 1435–1443.